CHAPTER VI

SYNTHESIS, GROWTH AND CHARACTERIZATION STUDIES OF SULPHAMIC ACID MIXED L-LACTIC ACID (SALA) UV NLO CRYSTAL

6. 1. Introduction:

Lactic acid known as milk acid where optically active isomers namely L(+)-lactic acid, and D(−)- lactic acid could form based on a chiral carbon atom attached with a hydroxyl group, and a carboxylic and a methyl groups are included (Narayanan 2004). Optical isomer lactic acid is industrially important and could be produced by fermentation (Martinez 2013). It gains the attention of researchers owing to its active chirality (Merlo 1993), biocompatibility and biodegradability (Lasprilla 2012), anti-corrosion (Ts, 2015), chemical feasibility (Xu 2016) and pharmaceuticability (Aljamal 2018). Lactic acid is used in crystal arthropathy. Lactic acid, Phosphoric acid and Trifluoroacetic acid could dissolve bone particulates of mineralized and demineralized forms but lactic acid only could form crystals. Microionized bone particulates could dissolve in lactic acid and directly generate calcium and phosphate containing crystals (Bulysheva 2018). Lactic acid was used as a precursor in order to enhance the spontaneous polarization of ferroelectric crystalline molecules (Otterholm 1987). It provides the chiral lactate ion which reveals peculiar ferroelectric, antiferroelectric orders and V-shaped electro-optic switching properties in liquid crystals (Wu 2005, Senthil 2008). L- lactic acid succeeds chiral precursor material (S)-2-octanol due to its low price and more stabilizing nature in thermal and chemical properties. Mesomorphic and structural properties of some liquid crystalline material consist of chiral lactate group possessing a blue phase, cholesteric, smectic phases

(Das 2012). Alkyl lactates are attracting precursors to synthesize chiral liquid crystals (Merlo 1993). Chiral active L- lactic acid was azeotropically esterificated with appropriate alcohols to produce optical active alkyl lactates (Bubnov 1999). Lactic acid based ligands are feasible to construct higher dimensional cadmium metalorganic framework crystals (Xu 2016).

Lactic acid and zinc oxide were mixed in stoichiometric ratio in aqueous solution to grow Zinc lactate trihydrate crystals at room temperature (Singh 1975), and Mn^{2+} doped Zinc lactate trihydrate crystals later (Kripal 2006). Ammonium borodilactate NLO crystal was grown by mixing ammonium carbonate, boric acid and lactic acid in1:2:4 ratio in water (Dhanuskodi 2003). Neodymium (Nd3+) doped ammonium borodilactate was grown by slow solvent evaporation technique (Panchanathan 2013). Lactic acid whey powder was mixed with deionized water and lactose crystals were dissolute under agitation (Mimouni 2007). Poly-L-lactic acid and poly-D-lactic acid were mixed at weight percentage in chloroform solution in order to prepare stereocomplex crystals (Tashiro 2017). In L-lactic acid aqueous solution, pyrrole and ammonium peroxodisulfate were mixed to prepare lactate colloidal particles (Okuno 2002). Incorporation of nano sized fillers enhances the functionality of poly-L-lactic acid (Krikorian 2004). The solubilities of magnesium-l-lactate, calcium-l-lactate, zinc-l-lactate, ferrous-l-lactate and aluminum-l-lactate in aqueous solution were determined (Apelblat 2005). Thermostable stereocomplex crystals based on PLLA were grown (Fujita 2008) by dispersion of grapheme oxide (Xu 2016) and boron nitride (Rosely 2018) nanosheets into poly-L-Lactic Acid. α-lactose monohydrate (α-LM) single crystal has been grown in the solvent mixtures of DMSO and Water in various ratio by both slow and fast evaporation technique.

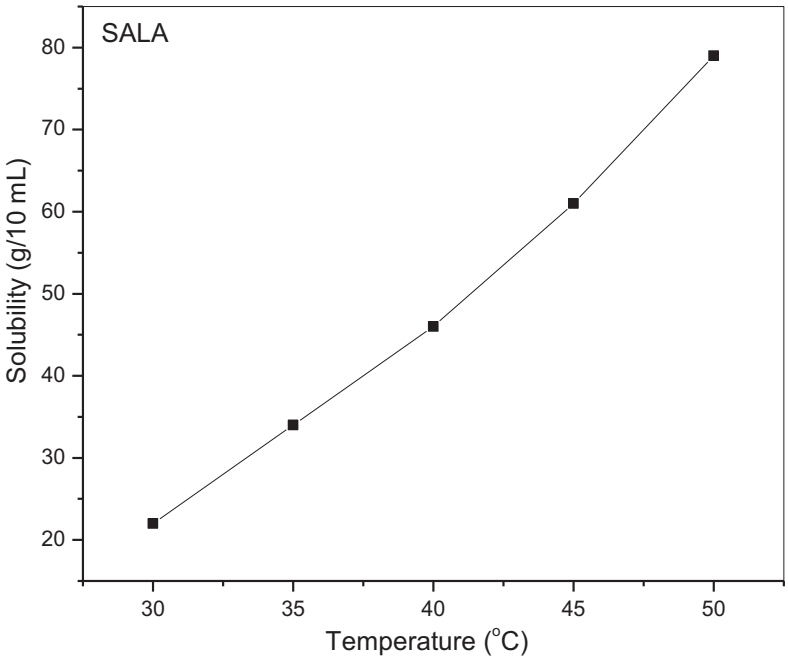

Fig. 6. 1. Solubility curve of SALA

Slow evaporation was recommended to grow α-LM with desired morphology (Vinodhini 2015). Copper lactate complexes in alkaline solutions (Achilli 2017) were prepared from Lactic acid mixed with $CuSO_4$ and K_2HPO_4. Calcium lactate crystal was harvested from the hydrothermal reaction of Calcium acetate and L-lactic acid in ethanol solution (Yang 2017). Recently Lactic acid and salicylic acid were stoichiometrically mixed in various solvents ethanol, methanol, diethyl ether and acetonitryl and co-crystals were obtained by reflux co-crystallization technique (Aljamal 2018). The L-lactic acid with its optical responses stimulate to synthesize and grow Sulphamic acid admixture L-Lactic acid (SALA) optical functional crystal for desired DUV NLO applications and to characterize its structural, optical, dielectric and mechanical properties.

6. 2. Experimental Techniques: SALA

6. 2. 1. Reagents

Sulphamic acid (Amino sulphonic acid) (99% pure AR grade) and L-lactic acid (99.5% pure AR grade) were purchased from E-merck Co Ltd.

6. 2. 2. Synthesis of SALA

Sulphamic acid was mixed equimolar with L-Lactic acid in a 250 mL borosil glass beaker. This mixture was stirred in water with the aid of magnetic stirrer at room temperature for 3 hrs and homogenized solution was obtained. The resultant solution was evaporated at NTP to yield Sulphamic acid mixed L-Lactic acid (SALA) seed crystals.

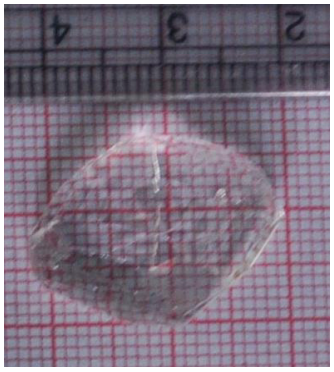

Fig. 6. 2. Photograph of as grown SALA UV NLO Crystal

6. 2. 3. Solubility study

To measure the solubility of SALA crystal in water, A 250 ml borosil glass beaker filled with 100 ml water was kept in constant temperature bath. An acrylic sheet with a circular hole at the middle covered the top of the beaker. A spindle from an electric motor, placed on the top of the sheet was introduced into the solution. A Teflon paddle attached at the end of the rod stirred the solution. The Crushed powder of SALA crystal was added in small amounts with water and stirring was continued till the solution attained supersaturation. A 20 ml of the saturated solution was withdrawn by means of a warmed pipette and the same was poured into a clean, dry and weighed Petri dish. The solution was kept in a heating mantle for slow evaporation till the whole of the solution got evaporated and the mass of the SALA salt in 20 ml of solution was determined by weighing the Petri dish with salt and hence the solubility, i.e quantity of salt in grams dissolved in 100 ml of the solvent was determined. The solubility of SALA in doubly deionized water was determined for five different temperatures (30, 35, 40, 45 and 50 ^{o}C) by adopting the same procedure. The resulting solubility curve of pure SALA is shown in Fig. 6.1.

6. 2. 4. Crystal growth technique

Seed crystals of SALA with good growth tendency were collected from the admixture solution and dissolved in doubly deionized water with the aid of magnetic stirrer till the solution saturated. The solution was filtered through Whatman filter paper. The filtered solution was collected in a beaker and allowed for slow evaporation by covering with pored acrylic sheet at top of the beaker. After 35-40 days, all solvent dried and SALA single crystals were grown at the bottom of the beaker.

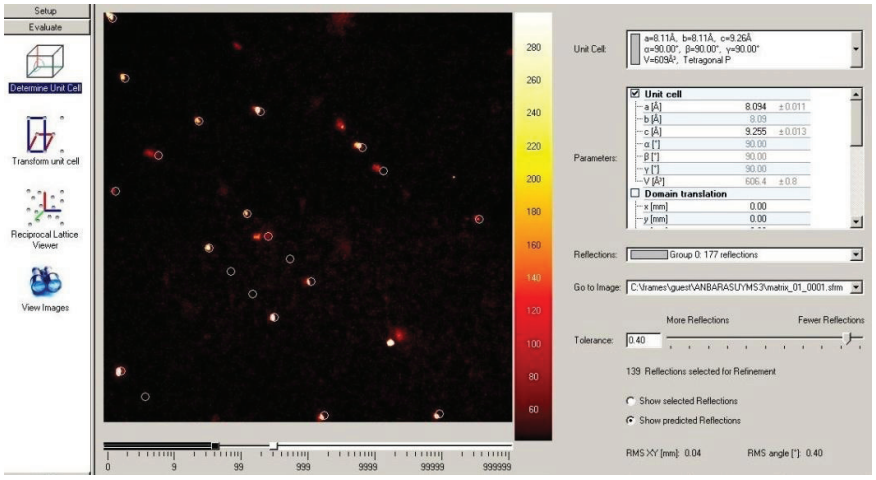

Fig. 6. 3. Single crystal XRD image of SALA UV NLO Crystal

Fig. 6. 2 displays the SALA crystal with a size of 23 x 22 x 10 mm^3 harvested from the aqueous solution. This facile route line materialized a UV transmittable NLO crystal Sulphamic acid mixed L-Lactic acid (SALA) grown in aqueous solution

6. 3. RESULTS AND DISCUSSION

SALA crystal was subjected to the following studies:

i. Single crystal X-ray Diffraction analysis (XRD) for measuring unit cell parameters.

ii. X-ray Powder Diffraction analysis (XRPD) to identify the crystalline phase with crystallinity.

iii. FTIR analysis to trace out the spectral map and confirm the various functional groups present in SALA molecule.

iv. UV-Vis-NIR analysis to study the optical absorption behavior of SALA crystal and to calculate its optical band gap energy.

v. Dielectric measurement technique to investigate the dielectric response of SALA for various frequency range

vi. Photoconductivity study to measure the photo responsiveness of the crystal

vii. NLO test was carried to check the SHG response of SALA

viii. The phase matching behavior of SALA crystalline medium was identified.

ix. Vicker's microhardness test to study the harness of the SALA crystal

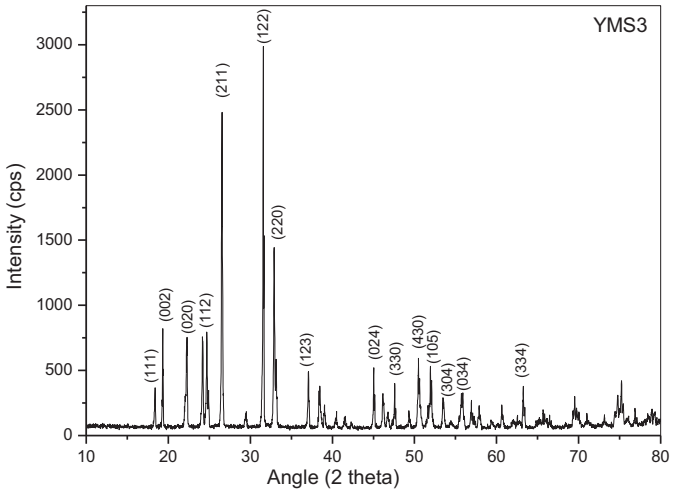

Fig. 6. 4. Powder XRD pattern of SALA UV NLO Crystal

6. 3. 1 Single Crystal X-Ray Diffraction analysis

Bruker AXS Kappa Apex II CCD Diffractometer equipped with graphite monochromated Mo (Kα) (λ = 0.71073 Å) radiation diagnosed the crystal structure of SALA. A suitable size SALA crystal fixed at the tip of the glass fiber using cyano acrylite adhesive was mounted on the goniometer head with the aid of video microscope and optically centered at the goniometer axes. The automatic cell determination routine, with 36 frames at three different orientations of the detector was employed to collect reflections for unit cell determination. Indexing and unit cell dimensions were found out using Apex2 software by difference vector method. Fig. 6. 3 screened the diagnostic report of SALA structure which reveals that SALA crystallized in Tetragonal P crystal system with unit cell parameters of a = 8.11 Å, b = 8.11 Å, c = 9.26 Å and α=β=γ =90°, and V = 609 $Å^3$. SALA molecule ordered in tetragonal P crystal system. Pure sulphamic acid crystallized in orthorhombic system (Kanda 1951), (Valluvan 2006). The modulator L-lactic acid distorted the structure of sulphamic acid from orthorhombic by equalizing two lattice parameters a and b.

6. 3. 2. Powder X-Ray Diffraction Analysis

Powder X-ray diffraction (PXRD) patterns were acquired with a XPERT-PRO powder diffractometer. Ground sample was placed on a quartz sample holder and was mounted on the diffractometer. Cu Kα radiation of wavelength λ = 1.5418 Å illuminate the sample and the resultant diffracted beams were collected over the range of 10–80^o with a scan speed of 0.2^o/s. Fig. 6. 4 displays the powder XRD pattern of SALA. The pure crystalline phases were identified their corresponding *hkl* plane values were manually indexed (Hesse 1948). It was observed that (122) plane highly diffracted at the Bragg's angle (2θ) of 31.56° with FWHM of 0.0612°.

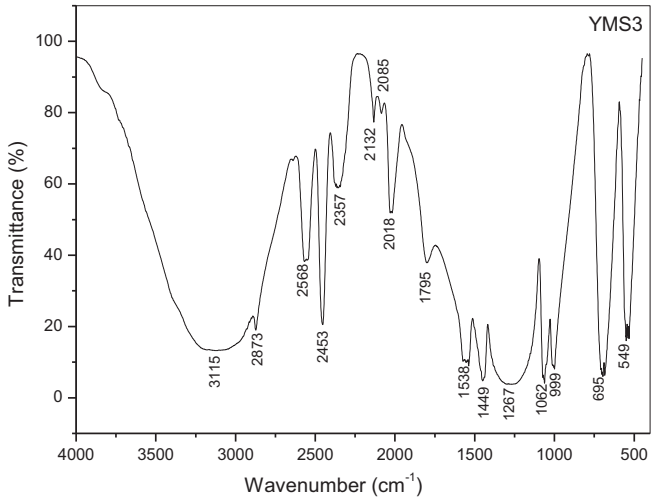

Fig. 6. 5. FTIR spectrum of SALA UV NLO Crystal

X-rays were diffracted at the planes (211) and (220) with Bragg's angle of 26.54° and 32.88° respectively. The peaks observed at various Bragg's angles with different intensity confirms the SALA crystal is a distorted structure from orthogonal of pure sulphamic acid crystal (Valluvan 2006), (Ramesh Babu 2010), (Thaila 2011) to tetragonal. This PXRD pattern confirms the existence of mixed crystal system of sulphamic acid and L-lactic acid.

6. 3. 3. FTIR analysis

FTIR spectrometer (Bruker model IFS 66 V) recorded the FTIR spectra of crushed SALA crystal powder embedded in KBr matrices in the range 400-4000 cm^{-1}. Fig. 6. 5 depicts the FTIR spectral map characterize the vibrations of the functional groups associated with sulphamic acid influenced by L-Lactic acid. The vibration of C-OH in carboxylic group and N-H stretching in amino group are combining at 3115 cm^{-1}. The peak at 1795 cm^{-1} is attributed to C=O symmetric stretching. The C-O is symmetrically stretching at 1267 cm^{-1}. A peak at 793 cm^{-1} is pertained to O-C-O bending. Asymmetrical stretching of CO_2^- was observed at 1538 cm^{-1}. Methyl CH_3 group asymmetrically bends at 1449 cm^{-1} and rocks at 999 cm^{-1}. C-CH_3 stretching was observed at 1062 cm^{-1}. Hydroxyl stretching was identified at 1004 cm^{-1}. N-H…O vibrates at 2873 cm^{-1}. NH_3^+ stretching put its spectrcal signature at 1449 cm^{-1} and 1570 cm^{-1}. The shift in standard absorption peaks of all functional moieties are reasoned with the mixed state of sulphamic acid and L-lactic acid acid in SALA molecule.

6. 3. 4. Optical Absorption study

Optical transmittance spectrum was recorded using Varian Cary 5E-UV-vis-NIR spectrometer in the wavelength region of 200 – 1400 nm.

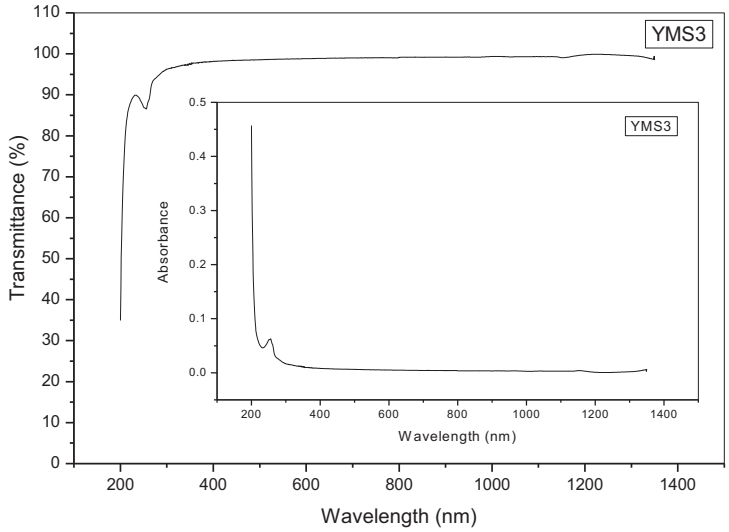

Fig. 6. 6. Optical transmittance of SALA UV NLO Crystal. The insert is the absorbance spectrum

Fig. 6. 6 depicts the optical transmittance spectrum showing SALA emanate UV radiation from 200 nm with short cut-off value of 228 nm. Wavelength increases from 200 nm to 210 nm, transmittance exponentially increases from 73to 95%. This is due to the chromophores are highly photosensitive to UV light. Transmittance of poly (L-Lactic acid) in UV region was 60% (Teoh 2017) and that of ammonium borodilactate was very low (Dhanuskodi, 2003). Pure and Nd^{3+} doped ammonium borodilactate was exhibit cut-off at 240nm and 230 nm respectively (Panchanathan 2013).

The optical absorption coefficient (α) was calculated from the transmittance using the relation

$$\alpha = (2.3036/d) \log(1/T) \quad \text{-------- (1)}$$

where d is the thickness of the crystal and T is the transmittance.

The optical band gap E_g is calculated from the Tauc's expression,

$$(\alpha h\nu)^n = A(h\nu - E_g) \quad \text{--------- (2)}$$

where α is the absorption coefficient, A is disorder parameter. E_g is calculated from the plot $(\alpha h\nu)^n$ versus hν. For the direct band gap energy n = 2 and for the indirect band gap energy n= (1/2). Fig. 6. 7 & Fig 6. 8 show the plot for direct transition and indirect transition respectively. From the graph it was observed that the direct band gap energy $E_{g(direct)}$ = 5.93 eV and indirect band gap energy $E_{g(indirect)}$ = 5.56 eV. Higher optical band gap energy value enhances the SALA crystal for laser generation and other NLO applications. The extinction coefficient of SALA crystal was plotted against the energy as shown in Fig. 6. 9 and the refractive index was plotted against wavelength as shown in Fig. 6. 10. SALA exhibits low extinction coefficient and low refractive indices in UV region.

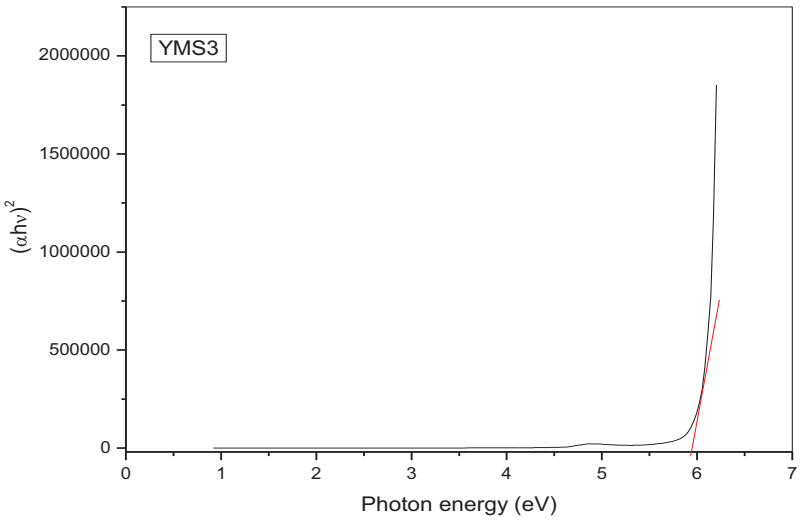

Fig. 6. 7. Tauc's Plot for direct optical band gap energy of SALA UV NLO Crystal

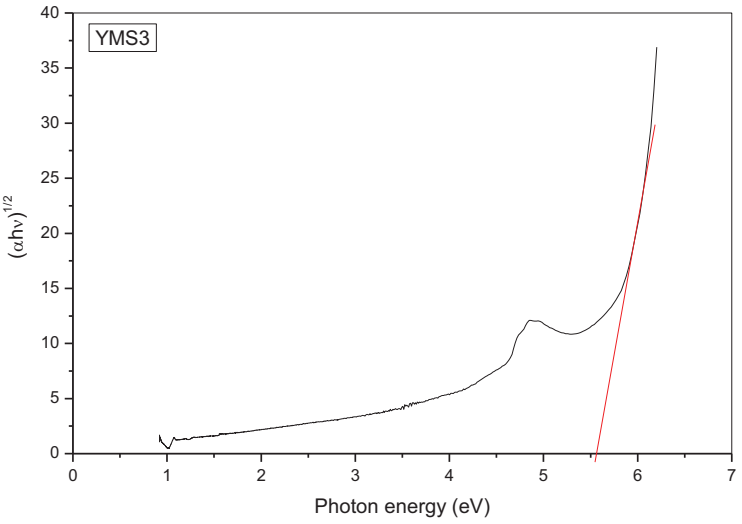

Fig. 6. 8. Tauc's Plot for indirect optical band gap energy of SALA UV NLO Crystal

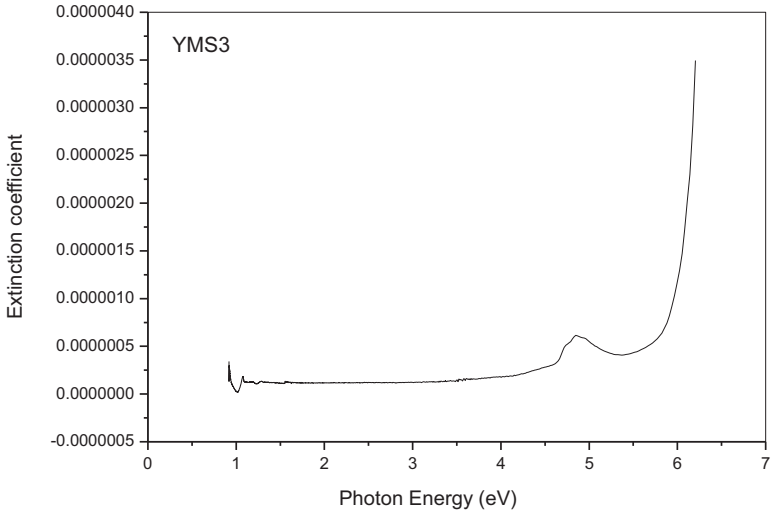

Fig. 6. 9. Plot of Extinction coefficient of SALA UV NLO Crystal

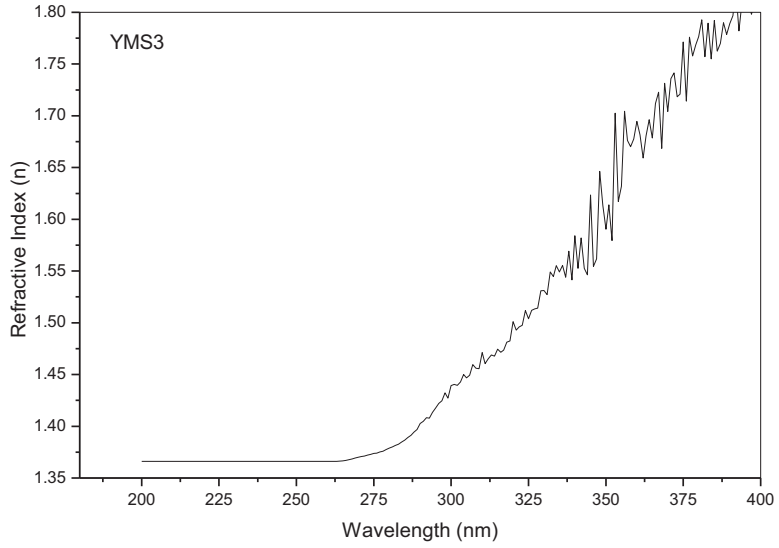

Fig. 6. 10. Plot of Refractive Index of SALA UV NLO Crystal

Wider UV transmittance window with low refractive index, low extinction coefficient and high optical band cap energy make SALA suitable for various optical applications.

6. 3. 5. Dielectric studies

Dielectric measurements for silver coated SALA crystal sample was carried out in the frequency range of 50 Hz to 5 MHz using Hioki 3532-50 LCR Hitester at various temperatures (40, 50, 60 ,70 ^{o}C). The plots of dielectric constant (ε_r) and dielectric loss (D) were drawn against frequency (log f) for different temperatures as shown in Fig. 6. 11 & Fig. 6. 12 respectively. SALA molecules polarized more when local electric field of low frequency induced them, due to the sum of space charge, dipolar, ionic and electronic polarizability. Optical responsive L-Lactic acid molecules excel the polarizabiliits. As the frequency of electric field increases, charge, dipolar, ionic polarizabity became ineffective except electronic polarizability and the relative permittivity of SALA decreases as well as dielectric loss. This normal dielectric sense of SALA discloses its charge transport mechanism and electric field distribution at all temperatures. The maximum values of dielectric constant of SALA at 50 Hz are measured as 6.33 9.36, 14.76and 16.09 at 40, 50, 60 and 70 ^{o}C respectively.

6. 3. 6. Photoconductivity study

Keithley 485 picoammeter measured the photoconductivity of SALA samples. Initially, the sample was kept away from any other radiations. The crystal sample was connected in series to a DC power supply and picoammeter. Silver paint was coated on sample to make the electrical contacts.

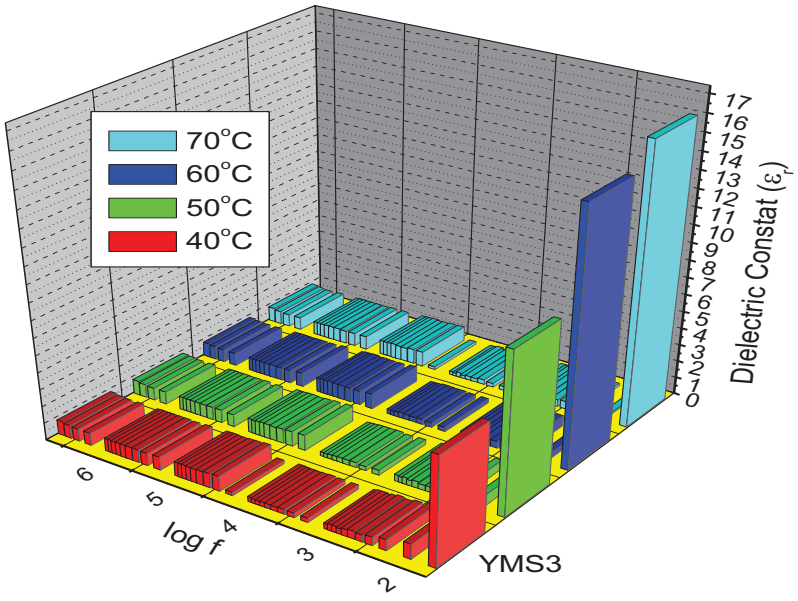

Fig. 6. 11. Plot of Dielectric constant of SALA UV NLO Crystal

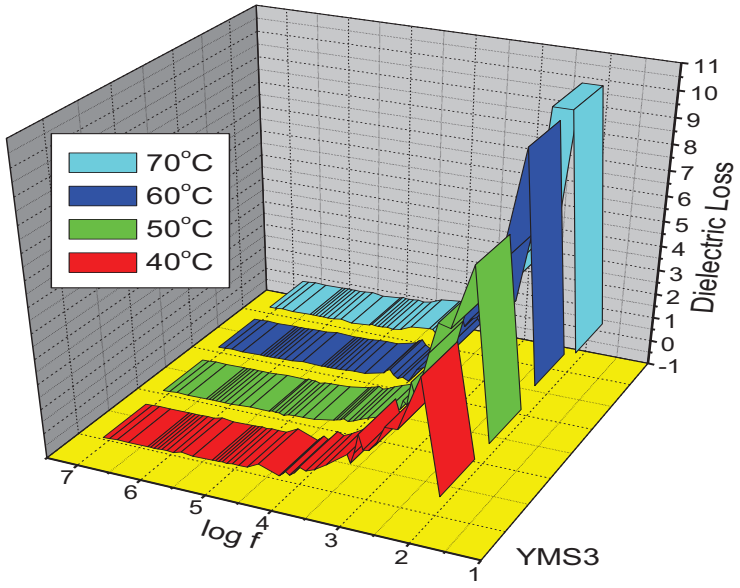

Fig. 6. 12. Plot of Dielectric loss of SALA UV NLO Crystal

The radiation from a halogen lamp containing iodine vapour was exposed on the sample by focusing a spot of light on the sample with the help of a convex lens. The photocurrent (I_p) was calculated. Initially the applied voltage was increased from 0 to 100 V in steps of 20 V and the corresponding dark currents were measured. Fig. 6. 13 depicts the plot of variation of both the dark current and photo current of the sample against the applied voltage. Both the dark and photocurrent were seen to increase linearly with the applied field. For the same applied field, the photo current is less than the dark current which reveals the negative photo conducting behaviour of SALA crystal.

6. 3. 7. NLO Test

In Kurtz-Perry powder test, Nd: YAG laser having fundamental radiation of 1064 nm with an input power 0.68 J as the optical source and illuminated on to the powdered sample of SALA through a visible blocking filter. a monochromator collected the 532 nm radiation after spreading the 1064 nm pump beam with an infrared blocking filter. SALA emanated second harmonics of primary Nd:YAG laser. Powder SHG efficiency was measured by a photomultiplier tube. A sample of KDP was used as a reference material for the present measurement. It is found that the SALA single crystal has an efficiency of 0.73 times that of KDP. It is greater than that of ammonium borodilactate having SHG efficiency of 0.552 with reference to KDP (Dhanuskodi, 2003).

6. 3. 8. Phase Matching analysis

SALA crystalline sample was ground and sieved into distinct particle sizes in the range of less than 106, 106-125, 125-150 and above 150 μm. KDP crystal was also sieved into the particle dimension of SALA.

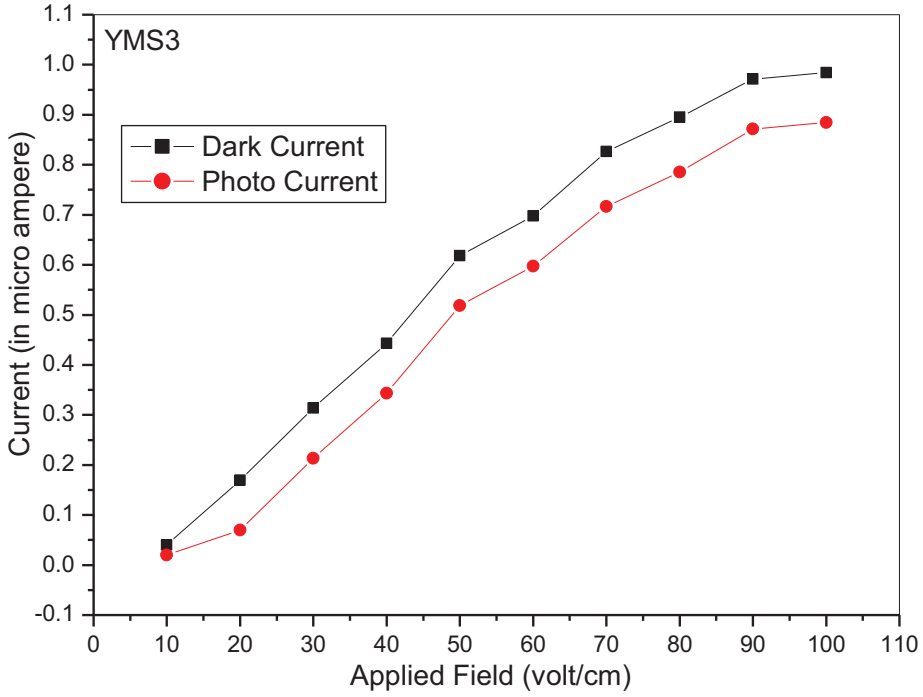

Fig. 6. 13. Photoconductivity of SALA UV NLO Crystal

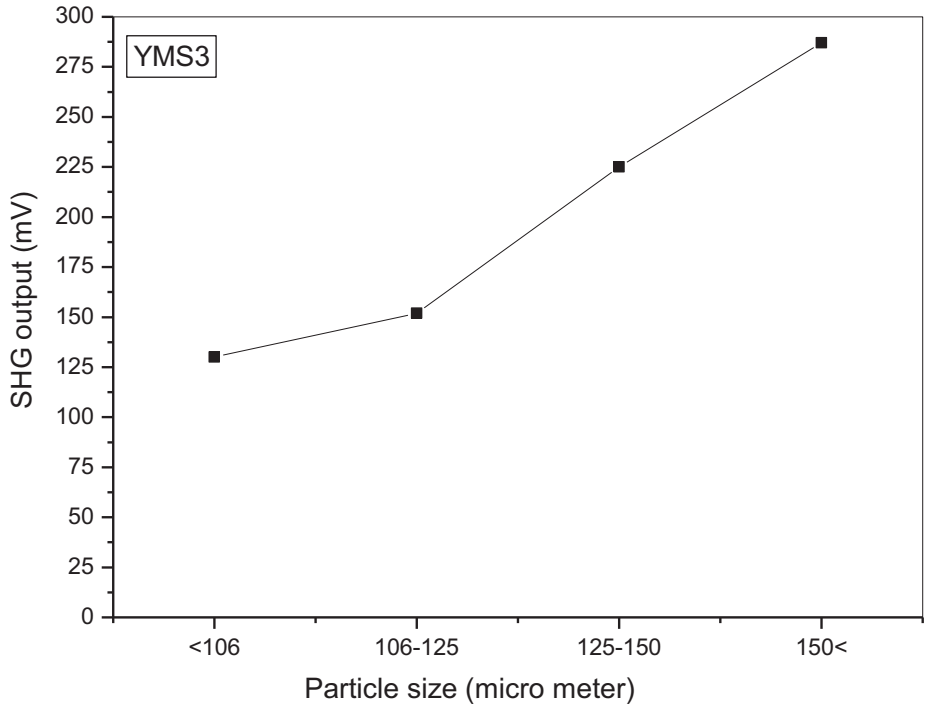

Fig. 6. 14. Phasematching curve of SALA UV NLO Crystal

Q-switched Nd:YAG infrared laser pulses irradiated on the sieves. SHG efficiency depends on the particle size and varies with size of sieves. SHG output was measured and plotted for various particle size. SHG intensities increased with increasing particle size upto 150 μm as shown in Fig. 6. 5. 14 promising the phase matching behavior of SALA. It is a promising phase matchable NLO crystal for LASER generation.

6. 3. 9. Microhardness study

Leitz Wietzlar Vickers Microhardness tester measured the hardness parameters of single crystal of SALA at room temperature. Flat shape crystal was fitted with a Vickers diamond pyramidal indenter light microscope. The static indentations were made at room temperature with a constant indentation time of 15 seconds for all indentation. The indenter marked on the crystal surfaces by varying the load from 20 to 100 g. The Vickers microhardness number H_v of the crystal was calculated using the relation

$$H_v = 1.8544\ P/d^2\ Kg\ mm^{-2} \quad \text{---------- (3)}$$

where P is the applied load and d is the average diagonal length of the indented impression in mm. Vickers microhardness profile as a function of load is shown in Fig. 6. 15. (a)

By using Meyer's law, the load P is related with the indentation size as

$$P = k_1 d^n \quad \text{---------- (4)}$$

Mayer constant (k_1) and work hardening coefficient (n) are the constants for a particular sample. The work hardening coefficient n is calculated from the slope of the curve drawn by plotting log (P) against log (d) as shown in Fig. 6. 15 (b)

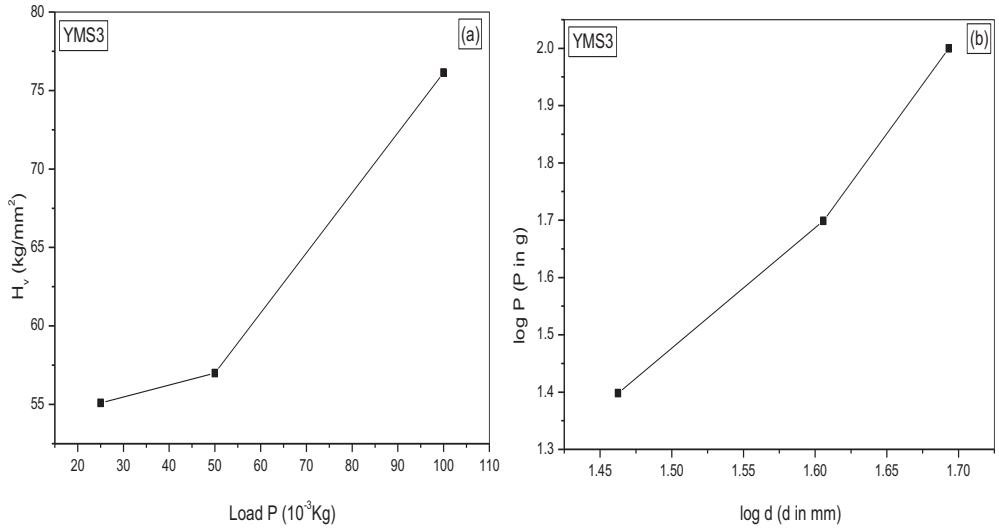

(a) Variation of hardness with load **(b) Plot of log P Vs log d**

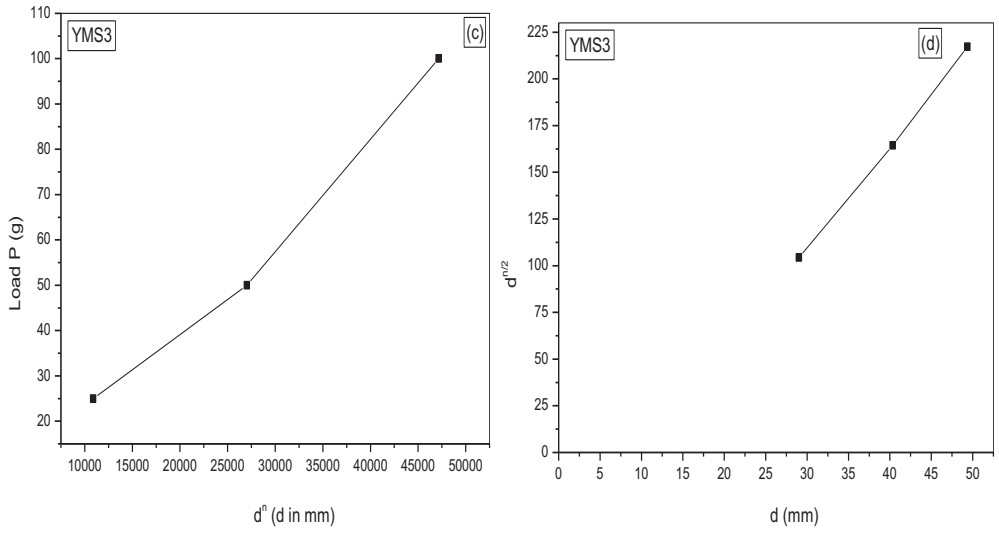

(c) Plot of d^n Vs P **(d) Plot of log d Vs $d^{n/2}$**

Fig. 6. 15. Microhardness measurements of SALA single crystal. (a) Variation of harness with load, (b) Plot of log P versus log d, (c) Plot of d^n versus P, (d) Plot of d versus $d^{n/2}$.

Table 6. 1. Hardness Parameters of SALA UV NLO Crystal

Hardness Parameters	Calculated Value
n	2.76
k_1	2.02 (10^{-3} Kg)
k_2	62.67 (10^{-3} Kg)
x	11 (μm)
σ_v	16.32 (MPa)

The value of k_1 was measured from the derivative of the curve drawn by plotting P against d^n as shown in Fig. 6. 15 (c). The value of n is found to be 2.45.

If n is greater than 2, the microhardness number H_v increases with increasing load (Onitsch 1947, Hanneman 1941), The work hardening coefficient value of SALA proves that SALA is a soft material.

The degree of dislocation density of the material is related with load P and indentation d through Kick's law given by

$$P = k_2(d+x)^2 \qquad \text{---------- (5)}$$

By simplifying Eqn. (4) and (5) we get

$$d^{n/2} = (k_2/k_1)^{1/2}\, d + (k_2/k_1)\, x \qquad \text{---------- (6)}$$

$d^{n/2}$ is plotted against d as shown in Fig. 6.15(d) and the slope of the straight line yields $(k_2/k_1)^{1/2}$ and the intercept is a degree of x.

The yield strength of the material is given by

$$\sigma_v = (H_v/2.9)\{[1-(2-n)] \times [(12.5)(2-n)/(1-(2-n))]^{2-n}\} \qquad \text{---------- (7)}$$

From the graphs, the constants k_1, k_2 and x are evaluated and the yield strength (σ_v) of SALA is computed. Hardness parameters of SALA crystal are tabulated in Table 6.1. As the work hardening coefficient value of SALA is n=2.45, it suggests that SALA is a soft material. The incorporation of phosphoric acid supported the soft growth habit and made it feasible to process.

6. 4. Conclusion

Sulphamic acid mixed L-Lactic acid crystal (SALA) was grown in aqueous solution by slow evaporation technique. The L-Lactic acid diverted sulphamic acid to be crystallized in Tetragonal crystal system. The functional groups of sulphamic acid and L-Lactic acid were confirmed by FTIR spectroscopy technique. Wider UV transmittance window starts with short cut-off at 228 nm. The optical band gap energy of SALA is 5.93 eV. UV light could travel through SALA crystal faster. The dielectric sense of SALA molecules was confirmed. SALA exhibits negative photo conducting behavior. It is a phase matchable second order NLO crystal. Chiral L-Lactic acid enhanced the SHG efficiency to 0. 73 times that of KDP. Soft crystal growth habit made it feasible to process. SALA is a UV transmittable crystal suitable for various energy harvesting processes.